Fast Spectrum Sensing with Coordinate System in Cognitive Radio Networks

Wilaiporn Lee, Kanabadee Srisomboon, and Akara Prayote

Spectrum sensing is an elementary function in cognitive radio designed to monitor the existence of a primary user (PU). To achieve a high rate of detection, most techniques rely on knowledge of prior spectrum patterns, with a trade-off between high computational complexity and long sensing time. On the other hand, blind techniques ignore pattern matching processes to reduce processing time, but their accuracy degrades greatly at low signal-to-noise ratios. To achieve both a high rate of detection and short sensing time, we propose fast spectrum sensing with coordinate system (FSC) — a novel technique that decomposes a spectrum with high complexity into a new coordinate system of salient features and that uses these features in its PU detection process. Not only is the space of a buffer that is used to store information about a PU reduced, but also the sensing process is fast. The performance of FSC is evaluated according to its accuracy and sensing time against six other well-known conventional techniques through a wireless microphone signal based on the IEEE 802.22 standard. FSC gives the best performance overall.

Keywords: Cognitive radio, spectrum sensing, principal component analysis.

Manuscript received June 7, 2014; revised Dec. 2, 2014; accepted Dec. 26, 2014.

This work was partially supported by the Thailand Research Fund (TRF) under grant number MRG5680101.

Wilaiporn Lee (corresponding author, wilaiporns@kmutnb.ac.th) and Kanabadee Srisomboon (s.kanabadee@gmail.com) are with the Electrical Engineering, Department of Electrical and Computer Engineering, the Faculty of Engineering, King Mongkut's University of Technology North Bangkok, Thailand.

Akara Prayote (akarap@gmail.com) is with the Department of Computer and Information Science, the Faculty of Applied Science, King Mongkut's University of Technology North Bangkok, Thailand.

I. Introduction

While the radio spectrum has become largely insufficient to those who demand its use, many already licensed bands remain underutilized [1]. The Federal Communications Commission (FCC) has considered providing unlicensed users with the opportunity to operate on a licensed spectrum in an opportunistic manner. Recently, cognitive radio (CR) [2]–[7] has emerged as a new communication technology aiming to solve the underutilization of spectrum resources by allowing unlicensed (secondary) users to dynamically utilize licensed bands that are left unused, without interference to licensed (primary) users. The first wireless access standard based on CR technology is that of TV white spaces in IEEE 802.22 [8]. Due to the legal rights of ownership surrounding the use of a spectrum band, a secondary user (SU) must vacate a band whenever a primary user (PU) reclaims its spectrum usage rights. The SU must be capable of knowing when the band is and is not available to them; that is, the presence and absence of a PU. Such a capability is known as spectrum sensing.

Three parameters are defined to evaluate the efficiency of spectrum sensing — accuracy of detection, computational complexity, and sensing time. The accuracy of detection is defined by the rate of correct detection of PUs when such users are actually present and occupying the spectrums concerned. This is a prime concern of spectrum sensing because a PU must not be affected by an SU. On the other hand, detecting the presence of a PU when in fact the PU is absent, otherwise known as false detection, has to be minimized to fully utilize spectrum bands. The accuracy of detection is usually shown in terms of a statistic; that is, in terms of a probability, which is often referred to as the probability of detection (P_d). Likewise, false detection is sometimes referred to as the probability of

false alarm (P_{fa}). In terms of the probability of detection, the higher the probability, the less likely it is that a PU will experience interference.

The second quality of service (QoS) parameter, computational complexity, is described by the computational burden. The complexity of a spectrum sensing technique affects both the amount of energy consumed by the technique during sensing and the latency of the technique. The higher the complexity, the higher the amount of energy consumed and the higher the latency, neither of which is desired. It generally comes at a cost when the spectrum sensing technique needs to improve its accuracy of detection.

The third QoS is sensing time, which is highly related to computational complexity. It should be noted that the computational complexity of a spectrum sensing technique can also be described by sensing time, since this is increased when the computational burden is increased. From the perspective of sensing time, the more channels an SU monitors, the more opportunities they will have of accessing a licensed band. In addition, an increase in sensing time will result in a decrease in an SU's throughput. It is stated in the IEEE 802.22 standard [9] that an SU needs to perform spectrum sensing within 2 s of a set sensing period with a false alarm probability of less than 0.1 and a detection probability higher than 0.9.

Generally, spectrum sensing techniques [10]–[24] can be classified into the following two groups: blind techniques and techniques based on prior knowledge of a signal. Blind techniques — energy detection (ED) [11]–[17], maximum eigenvalue detection (MED) [18], covariance absolute value (CAV) [18]–[20], and maximum to minimum eigenvalue (MME) detection [21]–[23] — determine the presence of PUs by measuring the energy or correlation of a received signal. Knowledge-based spectrum sensing techniques — matched filter detection (MFD) [11]–[15] and leading eigenvector detection (LED) [24] — require information on the patterns of signals from PUs to analyze observed signals. In general, knowledge-based techniques perform with higher accuracy than blind techniques. However, their computational burden and sensitivity to prior information are also higher than blind techniques. Furthermore, their performance is dependent upon on databases of patterns of PU signals; the pattern of a wireless microphone (WM) signal changes from one pattern to another in reality, even though it operates at the same frequency. The IEEE 802.22 standard categorized WM signals into three patterns — silent, soft speaker, and loud speaker [25]. If a new pattern belonging to a WM signal, one not yet in the database, is observed, then the accuracy of the knowledge-based techniques performances will drop. To keep track of all the possible patterns, large-sized databases are required, which in turn, would require the use of large memory spaces. It is factors such as these that will eventually result in a high computational time.

In this paper, a novel spectrum sensing algorithm, fast spectrum sensing with coordinate system (FSC), is proposed. The FSC algorithm is a knowledge-based technique, whereby the information of a PU is a prerequisite. The main difference from MFD and LED is that only significant features of original signals are used to construct a coordinate system. While these features reveal the intrinsic patterns of a PU, their dimension is much smaller than the original signal. To construct the new coordinate system, a feature-extraction process and feature-selection processes of a principal component analysis (PCA) [26]–[27] algorithm are adopted. To determine the existence of a PU, the FSC algorithm measures the percentage (weight) of correspondence between the received signal and a coordinate system. The magnitude of this weight will rise when a PU exists. Alternatively, it will fall when a PU does not exist. The FSC algorithm consumes little memory, requires little computational burden, and has a short sensing time.

In addition, this paper investigates the performance of six conventional spectrum sensing techniques — ED, MED, CAV, MME, MFD, and LED — with three WM signals. Most related literature focuses on detecting a specific pattern of WM signal; for example, an SU receiving only a silent WM signal. This paper provides a more comprehensive study in that it considers the fact that an SU can receive unpredictable patterns of a WM signal. The probability of detection and the sensing time are the two parameters used to evaluate the performance of spectrum sensing. The preliminary results show that MFD offers an accurate detection over a wide range of SNRs (–30 dB to 0 dB). On the other hand, ED gives the maximum number of sensing channels per sensing period (3,602 CHs/period). Thus, we use these evaluation results as a benchmark with which to compare the FSC algorithm. From the simulation results, it can be seen that the FSC algorithm performs spectrum sensing as fast as the ED technique while offering an accurate detection performance comparable to that of MFD.

In this paper, the following notation is used: superscript $(\bullet)^{T}$ and $(\bullet)^{*}$ stand for transpose and conjugate, respectively.

The remainder of this paper is organized as follows. Section II outlines the theoretical basis of spectrum sensing techniques, as well as providing a preliminary study on the effect of WM signal patterns on the performance of conventional spectrum sensing techniques. The framework for the FSC algorithm is presented in Section III. The simulation results and performance comparisons are shown in Section IV. Finally, conclusions are presented in Section V.

II. Related Study and Spectrum Sensing Techniques

This section gives a brief introduction to WM signals based on the IEEE 802.22 standard and conventional spectrum sensing techniques, as well as providing a preliminary study of the effect of the patterns of WM signals on the performance of conventional spectrum sensing techniques.

1. Spectrum Sensing Techniques

Spectrum sensing is a critical function of CR that periodically detects the existence of a PU during its sensing period. Generally, spectrum sensing techniques for transmitter detection can be broadly classified into the following two types: spectrum sensing techniques based on prior knowledge of a signal and blind spectrum sensing techniques. To detect the existence of a PU, there are two hypothesis models of a received signal that are expressed as follows:

$$\mathbf{x} = \begin{cases} \boldsymbol{\eta} & \text{when a PU is absent}\left[H_0\right], \\ \mathbf{s}+\boldsymbol{\eta} & \text{when a PU is present}\left[H_1\right], \end{cases} \tag{1}$$

where $\mathbf{x}$ is the signal an SU receives, $\boldsymbol{\eta}$ is additive white Gaussian noise (AWGN), and $\mathbf{s}$ is the signal transmitted by a PU. In general, the performance of a spectrum sensing technique can be evaluated through either a probability of detection or a probability of false alarm. A mathematical model of the various spectrum sensing techniques mentioned in this paper can be summarized as follows.

A. ED

Energy detection [11]–[17] is one of the most widely used techniques because it is easy to implement and does not require any prior knowledge of a signal's pattern. However, the performance of detection greatly degrades at low SNRs. Mathematical models of both $P_{\text{fa(ED)}}$ and $P_{\text{d(ED)}}$ are given by

$$Y_{\text{ED}} = \frac{1}{N}\sum_{n=1}^{N}\left|x(n)\right|^2, \tag{2}$$

where Y_{ED} and N denote the test statistic and the sample interval, respectively. The threshold is determined from the probability of false alarm ($P_{\text{fa(ED)}}$). In addition, the probability of detection ($P_{\text{d(ED)}}$) can also be used. Mathematical models of both the probability of false alarm and the probability of detection are given by

$$P_{\text{fa(ED)}} = Q\left[\left(\frac{\gamma_{\text{ED}}}{\sigma_{\eta}^{\,2}}-1\right)\sqrt{N}\right], \tag{3}$$

$$P_{\text{d(ED)}} = Q\left[\frac{\sqrt{N}}{\alpha+1}\left(\frac{\gamma_{\text{ED}}}{\sigma_{\eta}^{\,2}}-\alpha-1\right)\right], \tag{4}$$

$$\alpha = \frac{\sigma_{\mathbf{s}}^{\,2}}{\sigma_{\eta}^{\,2}}, \tag{5}$$

where γ_{ED} denotes the decision threshold, $Q(\cdot)$ is a standard Gaussian complementary cumulative distribution function, $\sigma_{\eta}^{\,2}$ is the variance of noise, and $\sigma_{\mathbf{s}}^{\,2}$ is the variance of a desired signal. To determine the existence of a PU, the test statistic (Y_{ED}) is compared to the decision threshold (γ_{ED}). The spectrum band is vacant if the test statistic is less than the threshold.

B. MFD

Matched filter detection [11]–[15] uses the correlation between the received and known signals. The output from MFD is compared to a threshold to determine the existence of a PU. The test statistic of MFD, Y_{MED}, is given by

$$Y_{\text{MFD}} = \sum_{n=0}^{N-1} x(n)s^{*}(n), \tag{6}$$

where $s^{*}(n)$ is the conjugate of the known signal. The decision threshold, γ_{MFD}, is determined from the probability of false alarm, $P_{\text{fa(MFD)}}$. Alternatively, the probability of detection, $P_{\text{d(MFD)}}$, can also be used as the decision threshold. Mathematical models for $P_{\text{fa(MFD)}}$ and $P_{\text{d (MFD)}}$ are given as

$$P_{\text{fa(MFD)}} = Q\left(\frac{\gamma_{\text{MFD}}}{\sigma_{\eta}\sqrt{E}}\right), \tag{7}$$

$$P_{\text{d(MFD)}} = Q\left(\frac{\gamma_{\text{MFD}}-E}{\sigma_{\eta}\sqrt{E}}\right), \tag{8}$$

where E is the energy of desired signal.

C. MED

Maximum eigenvalue detection [18] uses the maximum eigenvalue of the sample covariance matrix of the received signal. A received signal comprising L consecutive samples is given by

$$\mathbf{x} = \left[x(n)\,x(n-1),\ \ldots,\ x(n-L-1)\right]^{\text{T}}, \tag{9}$$

$$\mathbf{s} = \left[s(n)\,s(n-1),\ \ldots,\ s(n-L-1)\right]^{\text{T}}, \tag{10}$$

$$\boldsymbol{\eta} = \left[\eta(n)\eta(n-1),\ \ldots,\ \eta(n-L-1)\right]^{\text{T}}, \tag{11}$$

where L is a smoothing factor. Since the statistical covariance matrix cannot be directly calculated, the sample covariance matrix of the received signal is computed by the following procedure:

1) The sample auto-correlations of the received signal are

firstly expressed as

$$\varphi(l)=\frac{1}{N}\sum_{m=0}^{N-1}x(m)x(m-l),\qquad l=0,1,2,\ldots,L-1. \tag{12}$$

2) Secondly, the sample covariance matrix of the received signal is calculated as

$$\mathbf{R}_{\mathbf{x}}(N)=\begin{bmatrix}\varphi(0) & \varphi(1) & \cdots & \varphi(l-1)\\ \varphi(1) & \varphi(0) & & \varphi(l-2)\\ \vdots & \ddots & & \vdots\\ \varphi(l-1) & \cdots & & \varphi(0)\end{bmatrix}. \tag{13}$$

Note that the sample covariance matrix is a Toeplitz and symmetric matrix.

3) Thirdly, the eigenvalues of (13) are calculated using an eigen-decomposition algorithm. Note that only the maximum eigenvalue of the received signal, $\lambda_{\max}$, is used in step 4 to determine the existence of a PU.

4) Finally, the existence of a PU can now be determined from the value of $\lambda_{\max}$.

$$\lambda_{\max}(N)>\gamma_{\mathrm{MED}}\sigma_{\boldsymbol{\eta}}{}^{2}\quad\text{when a PU is present,} \tag{14}$$

$$\lambda_{\max}(N)\le\gamma_{\mathrm{MED}}\sigma_{\boldsymbol{\eta}}{}^{2}\quad\text{when a PU is absent,} \tag{15}$$

where γ_{MED} denotes a predetermined decision threshold.

Since the sample covariance matrix of the noise is nearly a Wishart random matrix, MED is analyzed using the probability distribution of the normalized largest eigenvalue — referred to as "Tracy–Widom distribution." Thereby, $P_{\mathrm{fa(MED)}}$ can be expressed as

$$P_{\mathrm{fa(MED)}}\approx 1-F\left(\frac{\gamma_{\mathrm{MED}}N-\rho}{v}\right), \tag{16}$$

$$\rho=\left(\sqrt{N-1}+\sqrt{L}\right)^{2}, \tag{17}$$

$$v=\left(\sqrt{N-1}+\sqrt{L}\right)\left(\frac{1}{\sqrt{N-1}}+\frac{1}{\sqrt{L}}\right)^{1/3}. \tag{18}$$

D. CAV Detection

With CAV [18]–[20], an SU determines the existence of a PU from the received signal. This is done by comparing the auto-correlation of the received signal to the CAV threshold. However, CAV will perform poorly when the auto-correlation of the received signal is low. The test statistic of CAV, Y_{CAV}, is given by

$$Y_{\mathrm{CAV}}=\left(\varphi(0)+\frac{2}{L}\sum_{l=1}^{L-1}(L-l)\left|\varphi(l)\right|\right)\left(\varphi(0)\right)^{-1}. \tag{19}$$

The threshold for CAV detection, γ_{CAV}, can be expressed as

$$\gamma_{\mathrm{CAV}}=\left(1+(L-1)\sqrt{\frac{2}{N\pi}}\right)\left(1-Q^{-1}P_{\mathrm{fa(CAV)}}\sqrt{\frac{2}{N}}\right)^{-1}. \tag{20}$$

A PU is present if $Y_{\mathrm{CAV}}\ge\gamma_{\mathrm{CAV}}$. Mathematical models for $P_{\mathrm{fa(CAV)}}$ and $P_{\mathrm{d(CAV)}}$ are given as

$$P_{\mathrm{fa(CAV)}}=1-Q\left[\frac{\frac{1}{\gamma_{\mathrm{CAV}}}\left(1+(L-1)\sqrt{\frac{2}{N\pi}}\right)-1}{\sqrt{\frac{2}{N}}}\right], \tag{21}$$

$$P_{\mathrm{d(CAV)}}=1-Q\left[\frac{\frac{1}{\gamma_{\mathrm{CAV}}}+\left(\frac{\gamma_{L}\mathrm{SNR}}{\gamma_{\mathrm{CAV}}(\mathrm{SNR}+1)}\right)-1}{\sqrt{\frac{2}{N}}}\right], \tag{22}$$

where γ_{L} is given by

$$\gamma_{L}\triangleq\frac{2}{L}\sum_{l=1}^{L-1}(L-1)\left|\alpha_{l}\right| \tag{23}$$

and α_{l} is given by

$$\alpha_{l}=E\left[s(n)s(n-l)\right]\Big/\sigma_{\mathbf{s}}{}^{2}. \tag{24}$$

E. MME

The procedure of MME [21]–[23] is similar to MED. However, the MME method determines the existence of a PU by comparing the ratio of the maximum and minimum eigenvalues with the threshold γ_{MME}. MME detection can be calculated using (13). The test statistic for the MME detection method is given by

$$Y_{\mathrm{MME}}=\lambda_{\max}\Big/\lambda_{\min}. \tag{25}$$

The probability of false alarm for MME detection is given by

$$P_{\mathrm{fa(MME)}}\approx 1-F\left[\frac{\gamma_{\mathrm{MME}}\left(\sqrt{N}+\sqrt{L}\right)^{2}-\rho}{v}\right]. \tag{26}$$

F. LED

Leading eigenvector detection [24] calculates the correlation between the leading eigenvector of the received signal and the leading eigenvector of the known signal. The output is compared to a threshold to determine the existence of a PU. Since LED keeps only the most significant feature of the received signal, the technique requires less memory than MFD. However, since the LED technique needs to calculate the leading eigenvector of the received signal, the sensing time and complexity of computation is increased. Let us define the

following PU signals, $\mathbf{x}_i, i = 1, 2, \ldots, M$, each of which have d dimensions, as

$$\begin{aligned} \mathbf{x}_1 &= \left[x(n)x(n+1)\cdots x(n+d-1)\right]^{\mathrm{T}}, \\ \mathbf{x}_2 &= \left[x(n+1)x(n+2)\cdots x(n+d)\right]^{\mathrm{T}}, \\ &\vdots \\ \mathbf{x}_M &= \left[x(N+n-d)\cdots x(N+n-1)\right]^{\mathrm{T}}. \end{aligned} \tag{27}$$

The LED procedure can then be summarized as follows:

1) The sample covariance matrix of a received signal $\mathbf{x}_i$ is given by

$$\mathbf{R}_{\mathbf{x}} = \frac{1}{M}\sum_{i=1}^{M}\mathbf{x}_i\mathbf{x}_i^{\mathrm{T}}. \tag{28}$$

Note that we assume the sample mean to be zero.

2) The eigenvalues and eigenvectors of the received signal can be calculated using (28). Only an eigenvector corresponding to the largest eigenvalue, $\mathbf{v}_1$, is considered. The test statistic for LED is given by

$$Y_{\mathrm{LED}} = \max_{l=0,1,2,\ldots,d}\left|\sum_{j=1}^{d}\mathbf{v}_1[j]\hat{\mathbf{v}}_1[j+l]\right|. \tag{29}$$

3) The existence of a PU can now be determined from the value of Y_{LED}.

$$Y_{\mathrm{LED}} > \gamma_{\mathrm{LED}} \quad \text{when a PU is present,} \tag{30}$$

$$Y_{\mathrm{LED}} \le \gamma_{\mathrm{LED}} \quad \text{when a PU is absent,} \tag{31}$$

where $\hat{\mathbf{v}}_1$ is the leading eigenvector of the received signal, $\mathbf{v}_1$ is the leading eigenvector of the known signal, and γ_{LED} is a predetermined threshold.

2. Preliminary Experiments

As mentioned in Section I, the pattern of a received WM signal may change despite the fact that it operates at the same carrier frequency. In this section, we evaluate the performance of six conventional spectrum sensing techniques — ED, MED, CAV, MME, MFD, and LED — under the assumption that a received WM signal has a randomly occurring pattern. Two important factors — P_{d} and sensing time of each technique — are considered in our performance evaluation.

An AWGN is used as a communication channel between a PU and an SU. Based on IEEE 802.22 [25], PU's transmitted signal can be expressed as

$$s(t) = A_{\mathrm{c}}\cos\left(2\pi f_{\mathrm{c}}\mathrm{t} + 2\pi k_{\mathrm{f}}\int_0^t m(\tau)\,\mathrm{d}\tau\right), \tag{32}$$

$$m(\tau) = \sin(f_{\mathrm{m}}t), \tag{33}$$

Table 1. Model of WM signal model [25].

	Silent	Soft speaker	Loud speaker
$m(\tau)$ frequency (kHz)	32	3.9	13.4
FM deviation factor (kHz) (k_{f})	±5	±15	±32.6

Table 2. Different knowledge bases of PU signal known to an SU.

Case	Description
1	Silent of WM signal is known by SU.
2	Soft speaker of WM signal is known by SU.
3	Loud speaker of WM signal is known by SU.
4	All three patterns of WM signal are known by SU.

where A_{c} is the amplitude of a carrier signal, $m(\tau)$ is a modulating signal, f_{m} is message frequency, f_{c} is carrier frequency, and k_{f} is a frequency modulation (FM) deviation factor. The values of both the modulating signal $m(\tau)$ and the FM deviation factor k_{f} (see Table 1) represent the three different patterns of a WM signal; that is, silent, soft speaker, and loud speaker. To study spectrum sensing performance under different levels of knowledge, the SU is equipped with four different knowledge bases, as described in Table 2.

The simulation results of six conventional spectrum sensing techniques — ED, MED, CAV, MME, MFD, and LED — are shown in Table 3. As four of the six techniques — ED, MED, CAV, and MME — are blind techniques, their detection performances will not be affected by different knowledge bases. Hence, the individual results of these blind techniques are not shown; rather, they are shown collectively due to the fact that they have similar detection performances. On the other hand, different knowledge bases greatly affect the detection performances of the knowledge-based techniques — MFD and LED.

Figure 1 shows the simulation results of MFD and LED for the four cases outlined in Table 2. The graph plots P_{d} as a function of SNR. It is clear that the detection performance of MFD is greatly affected by the knowledge base of PU's signal. When SU observes a pattern of WM signal that is not in the knowledge base, the detection performance of MFD greatly degrades.

As depicted in the figure, the detection performance of LED in cases 1–4 is shown using only a single line. This is because the detection performances were practically identical to each other, due to the fact that the leading eigenvectors of the WM signal patterns were similar to each other. Thus, the detection performance of LED was not affected by a difference in WM

Table 3. Performance comparison of conventional spectrum sensing techniques.

Sensing technique			Prior knowledge			Ability to detect WM signal		
			Waveform pattern	Noise power	Memory (kbytes)	Critical SNR ($P_d \geq 0.9$)	Average sensing time (ms)	Channels/sensing period of 2 s
Blind spectrum sensing	ED		×	✓	0	–16 dB	0.04997	3,602
	MED		×	✓	0	–16 dB	2.6	69
	CAV		×	×	0	–16 dB	2.5	72
	MME		×	×	0	–16 dB	2.9	62
Spectrum sensing based on prior knowledge	MFD	Case 1	✓	✓	40	–8 dB	2.5	72
		Case 2	✓	✓	40	–30 dB	2.5	72
		Case 3	✓	✓	40	–30 dB	2.5	72
		Case 4	✓	✓	120	–30 dB	5.4	33
	LED	Case 1	✓	✓	0.192	–18 dB	78.09	2
		Case 2	✓	✓	0.064	–18 dB	78.09	2
		Case 3	✓	✓	0.064	–18 dB	78.09	2
		Case 4	✓	✓	0.192	–18 dB	80.70	2

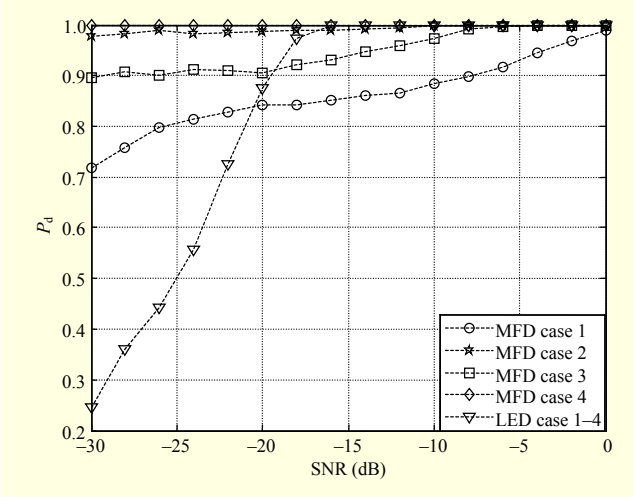

Fig. 1. Detection performance of MFD and LED under different received WM signal cases.

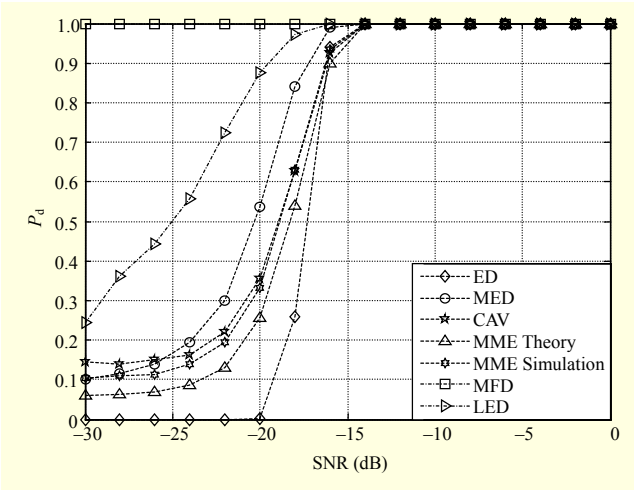

Fig. 2. Performance comparison of conventional spectrum sensing techniques when patterns of PU signal are known.

signal pattern. However, LED inflicts a high computational burden upon the SU when performing spectrum sensing; thus, the associated sensing time is often substantial.

Figure 2 shows the performance comparison of conventional spectrum sensing techniques when the patterns of WM signals are known. MFD offers the best detection performance among the spectrum sensing techniques. When evaluating the performance of MME, the calculated MME threshold (theoretical), γ_{MME}, offers an implausible performance at low SNRs.

In [20], the authors improve the detection performance of MME by finding new thresholds through Monte Carlo simulations. To compare the performance of MME under the different types of thresholds (theoretical and Monte Carlo simulations), we present the performance of "MME Theory" and "MME Simulation" in Fig. 2. Note that "MME Theory" denotes experimental results where the threshold is calculated from a theoretical formula. "MME Simulation" denotes experimental results where the threshold is estimated through Monte Carlo simulations.

Table 3 gives a performance comparison of the conventional spectrum sensing techniques for various cases of prior knowledge. The SNR required of a spectrum sensing technique to meet the required accuracy of detection (that is, $P_d \geq 0.9$) [9],

is given in the "Critical SNR" column of Table 3. The lower the "Critical SNR" value, the more tolerant to noise the technique is. From Table 3, the knowledge-based spectrum sensing techniques — MFD and LED — are confirmed to be more tolerant to noise than the blind techniques.

On the other hand, the average sensing time shown for each technique is based on the average from the Monte Carlo simulations. As shown in Table 3, ED consumes the least average sensing time, whereas LED consumes the longest average sensing time. These average sensing time values are used as a benchmark when evaluating the average sensing time of the FSC algorithm.

Moreover, the results in Table 3 show that ED offers the maximum number of channels per sensing period. However, there is no standard or requirement that defines the minimum number of channels that should be monitored in a given sensing period. If the number of channels per sensing period increases, then the SU will have more opportunities to utilize the unused licensed band.

III. FSC

In this section, the FSC algorithm is described in detail with mathematical models. The FSC algorithm is a spectrum sensing technique that requires prior knowledge of a PU's signals. The framework for the FSC algorithm can be categorized into two phases — coordinate system construction and sensing. The coordinate system must be predetermined from the two most significant features of WM signals and kept in the knowledge base. The sensing phase determines the existence of a PU by comparing the FSC decision statistic (Y_{FSC}) to the FSC threshold (γ_{FSC}). The decision statistic is calculated by projecting the PU's signal onto the predetermined coordinate system.

1. Coordinate System Construction

In this section, our coordinate system is introduced. The new coordinate system is of a lower dimension than the original data space. The main objectives of this phase are to select the two most significant features of WM signals and to construct a coordinate system. Our coordinate system construction process (as shown in Fig. 3) exploits the feature extraction and selection process of a PCA algorithm [26]–[27] to filter out the two most significant features of WM signals and then uses them as the axes for a new coordinate system. Due to the smaller size of the new coordinate system, the FSC algorithm consumes less memory, has less computational burden, and has a short sensing time.

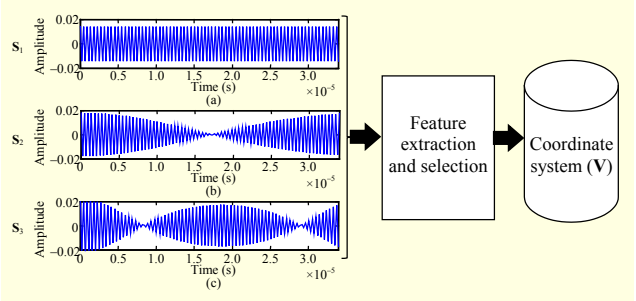

Fig. 3. Coordinate system construction phase of FSC algorithm.

We assume that the WM signals of a PU are known to an SU. These WM signals are used as the *training* signals. Let the vectors $\mathbf{s}_1$, $\mathbf{s}_2$,⋯, $\mathbf{s}_M$ represent WM signals. These vectors are referred to as *training* vectors. The training vectors are given by

$$\begin{aligned}\mathbf{s}_1 &= [s_1(1)s_1(2)\cdots s_1(N)]^{\mathrm{T}},\\ \mathbf{s}_1 &= [s_2(1)s_2(2)\cdots s_2(N)]^{\mathrm{T}},\\ &\vdots\\ \mathbf{s}_M &= [s_M(1)s_M(2)\cdots s_M(N)]^{\mathrm{T}}.\end{aligned} \tag{34}$$

The procedure for the coordinate system construction phase is described as follows.

A. Feature Extraction

Firstly, we eliminate the common features of the WM signals by subtracting the average WM signals vector ($\boldsymbol{\varepsilon}$) from each training vector ($\mathbf{s}_i$).

$$\boldsymbol{\beta}_i = \mathbf{s}_i - \boldsymbol{\varepsilon}, \tag{35}$$

where $\boldsymbol{\beta}_i$ is a vector that contains the significant features of the WM signals. The average WM signals vector ($\boldsymbol{\varepsilon}$) can be expressed as

$$\boldsymbol{\varepsilon} = \frac{1}{M}\sum_{i=1}^{M}\mathbf{s}_i. \tag{36}$$

Next, we compute the covariance matrix ($\mathbf{C}$) of $\boldsymbol{\beta}_i$, which is given by

$$\mathbf{C} = \frac{1}{M}\sum_{i=1}^{M}\boldsymbol{\beta}_i\boldsymbol{\beta}_i^{\mathrm{T}}. \tag{37}$$

From the covariance matrix, a matrix of eigenvectors ($\mathbf{V} = [\mathbf{v}_1\mathbf{v}_2\ldots\mathbf{v}_d]$) and a vector of corresponding eigenvalues ($\boldsymbol{\lambda} = [\lambda_1\lambda_2\ldots\lambda_d]^{\mathrm{T}}$) can be obtained by using the aforementioned eigen-decomposition algorithm.

B. Feature Selection

From the matrix of eigenvectors ($\mathbf{V}$), we keep only the *k best* eigenvectors (that is, those that correspond to the k largest eigenvalues), and the resulting set is then used to form the new

coordinate system. The k best eigenvectors are determined by

$$\sum_{i=1}^{k}\lambda_i \Big/ \sum_{i=1}^{d}\lambda_i \geq 95\%, \tag{38}$$

where d is the number of eigenvalues in set λ.

It is clear that 95% of the total number of features present in the WM signals is a sufficient amount to be representative of all the existing features. Hence, having decided to only select the k best eigenvectors, the dimension of the WM signals is reduced. Reducing the dimension of the WM signals avoids a huge amount of computational burden. Moreover, the effect of noise from the original signal is avoided due to the reduction in dimension of the WM signals. Furthermore, the FSC algorithm is tolerant to noise.

2. Sensing Phase

In the sensing phase (see Fig. 4), the weight of correspondence between the received WM signal and the new coordinate system is calculated by projecting the received signal onto the coordinate system. This weight describes the distribution of the received signal in the new coordinate system. The weight, given as a vector $(\hat{\mathbf{x}})$, can be expressed as

$$\hat{\mathbf{x}} = \mathbf{V}^{\mathrm{T}}(\mathbf{x}-\boldsymbol{\varepsilon}). \tag{39}$$

The magnitude of the weight vector is defined as the FSC decision statistic (Y_{FSC}). The magnitude of the weight vector will rise when a PU is present. Otherwise, the magnitude of the weight vector will fall when a PU is not present. The FSC decision statistic (Y_{FSC}) can be expressed as

$$Y_{\mathrm{FSC}} = \|\hat{\mathbf{x}}^2\| = \left(\sqrt{\sum_{i=1}^{k}(\hat{\mathbf{x}})^2}\right)^2 = \sum_{i=1}^{k}(\hat{\mathbf{x}})^2. \tag{40}$$

A mathematical model for the probability of false alarm of the FSC algorithm is given by

$$P_{\mathrm{fa(FSC)}} = P\left[Y_{\mathrm{FSC}} \geq \gamma_{\mathrm{FSC}} \mid H_0\right]. \tag{41}$$

Under condition H_0,

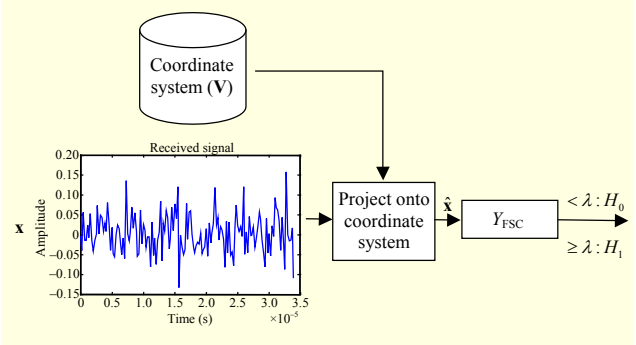

Fig. 4. Sensing phase of FSC algorithm.

$$\hat{\mathbf{x}}_{\boldsymbol{\eta}} = \mathbf{V}^{\mathrm{T}}(\mathbf{x}_{\boldsymbol{\eta}}-\boldsymbol{\varepsilon}). \tag{42}$$

$$Y_{\mathrm{FSC}} = \|\hat{\mathbf{x}}_{\boldsymbol{\eta}}\|^2 = \left(\sqrt{\sum_{i=1}^{k}(\hat{\mathbf{x}}_{\boldsymbol{\eta}})^2}\right)^2 = \sum_{i=1}^{k}(\hat{\mathbf{x}}_{\boldsymbol{\eta}})^2, \tag{43}$$

$$\mu_{H_0} = \mathrm{E}\left[Y_{\mathrm{FSC}}\right] = \mathrm{E}\left[\sum_{i=1}^{k}(\hat{\mathbf{x}}_{\boldsymbol{\eta}})^2\right] = k\mathfrak{m}'_{2,H_0}, \tag{44}$$

$$\sigma^2_{H_0} = \mathrm{Var}\left[\sum_{i=1}^{k}(\hat{\mathbf{x}}_{\boldsymbol{\eta}})^2\right] = k\left(\mathfrak{m}'_{4,H_0} - \left(\mathfrak{m}'_{2,H_0}\right)^2\right), \tag{45}$$

$$P_{\mathrm{fa(FSC)}} = Q\left(\frac{\gamma_{\mathrm{FSC}} - k\mathfrak{m}'_{2,H_0}}{\sqrt{k\left(\mathfrak{m}'_{4,H_0} - \left(\mathfrak{m}'_{2,H_0}\right)^2\right)}}\right). \tag{46}$$

Note that μ_{H_i} is the mean value of H_i and that $\mathfrak{m}'_n$ is the nth order moment of the FSC decision statistic (Y_{FSC}).

Similar to the probability of false alarm, the probability of detection for the FSC algorithm can be expressed as

$$P_{\mathrm{d(FSC)}} = P\left[Y_{\mathrm{FSC}} \geq \gamma_{\mathrm{FSC}} \mid H_1\right]. \tag{47}$$

Under condition H_1,

$$\hat{\mathbf{x}}_{\mathbf{s}+\boldsymbol{\eta}} = \mathbf{V}^{\mathrm{T}}(\mathbf{x}_{\mathbf{s}+\boldsymbol{\eta}}-\boldsymbol{\varepsilon}), \tag{48}$$

$$Y_{\mathrm{FSC}} = \|\hat{\mathbf{x}}_{\mathbf{s}+\boldsymbol{\eta}}\|^2 = \left(\sqrt{\sum_{i=1}^{k}(\hat{\mathbf{x}}_{\mathbf{s}+\boldsymbol{\eta}})^2}\right)^2 = \sum_{i=1}^{k}(\hat{\mathbf{x}}_{\mathbf{s}+\boldsymbol{\eta}})^2, \tag{49}$$

$$\mu_{H_1} = \mathrm{E}\left[Y_{\mathrm{FSC}}\right] = \mathrm{E}\left[\sum_{i=1}^{k}(\hat{\mathbf{x}}_{\mathbf{s}+\boldsymbol{\eta}})^2\right] = k\mathfrak{m}'_{2,H_1}, \tag{50}$$

$$\sigma^2_{H_1} = \mathrm{Var}\left[\sum_{i=1}^{k}(\hat{\mathbf{x}}_{\mathbf{s}+\boldsymbol{\eta}})^2\right] = k\left(\mathfrak{m}'_{4,H_1} - \left(\mathfrak{m}'_{2,H_1}\right)^2\right), \tag{51}$$

$$P_{\mathrm{d(FSC)}} = Q\left(\frac{\gamma_{\mathrm{FSC}} - k\mathfrak{m}'_{2,H_1}}{\sqrt{k\left(\mathfrak{m}'_{4,H_1} - \left(\mathfrak{m}'_{2,H_1}\right)^2\right)}}\right). \tag{52}$$

In addition, the probability of misdetection of the FSC algorithm is given by

$$P_{\mathrm{m(FSC)}} = 1 - P_{\mathrm{d(FSC)}}. \tag{53}$$

IV. Simulation Results

In this section, we give the simulation results of eight spectrum sensing techniques. The transmitted PU signals are assumed to be WM signals, based on IEEE 802.22, whereby the patterns of the WM signals are assumed to be in the

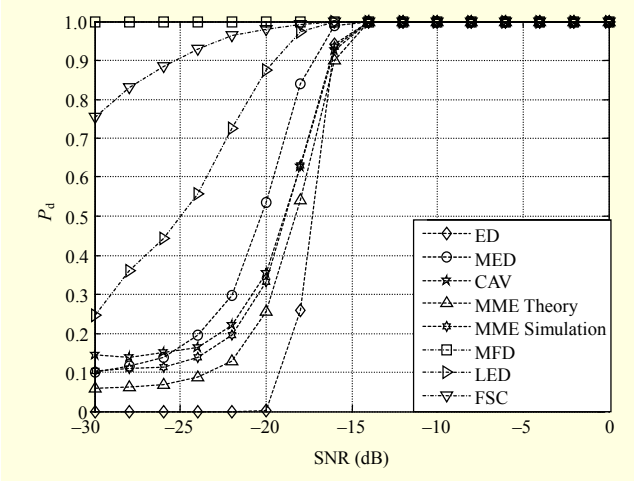

Fig. 5. Probability of detection vs. SNRs of ED, MED, CAV, MME, MFD, LED, and FSC.

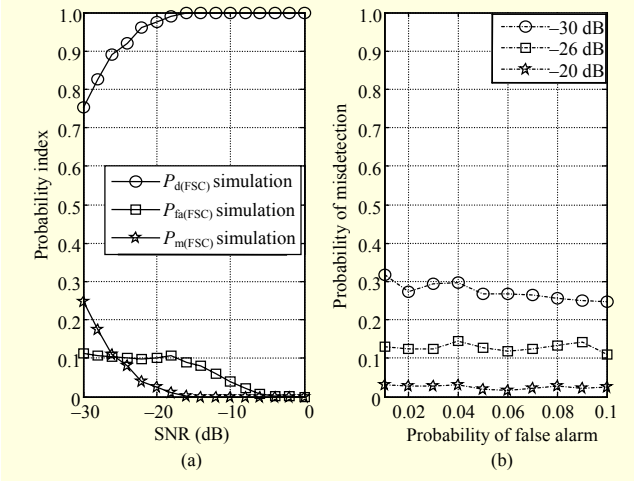

Fig. 6. Performance of FSC algorithm.

knowledge base of the SU. The parameters of the WM signals are shown in Table 1. A single received WM signal is assumed to contain one of three randomly occurring patterns. The communication channel between the transmitter and the receiver is assumed to be an AWGN channel, and the SNR at the receiver is assumed to be between –30 dB and 0 dB. The other parameters that were used in the simulations took the following values: n = 5,000; L = 10; and P_{fa} = 0.1. All the experiments are performed under Windows 7 and MATLAB running on a PC equipped with an Intel Dual-Core CPU at 2.93 GHz and 4 GB RAM memory.

As depicted in Fig. 5, the FSC algorithm gives a better detection performance than the other conventional spectrum sensing techniques, except MFD, which is known as the optimum spectrum sensing technique. The critical SNR of the FSC algorithm is –24 dB (see Table 4). From the perspective of sensing time, the FSC algorithm consumes less sensing time than the other conventional techniques, except ED (see Table 4). The reason for this is that the FSC algorithm performs spectrum sensing with little computational burden due to the small size of the weight vector ($\hat{\mathbf{x}}$). Calculated from the averaged sensing time of FSC, the FSC algorithm can sense 3,370 channels per sensing period. When compared with the results in Table 3, we can see that the FSC algorithm can perform spectrum sensing with a number of communication channels that rivals that of ED.

To validate the performance of the FSC algorithm, graphs of $P_{d(FSC)}$, $P_{m(FSC)}$, and $P_{fa(FSC)}$ are shown in Fig. 6(a). In this figure, as SNR increases, $P_{d(FSC)}$ increases while $P_{m(FSC)}$ and $P_{fa(FSC)}$ decrease. The simulation results are as we expected, and this is explained as follows. By projecting the received signal to the proposed coordinate system, we obtained the weight vector and weight of correspondence between the received signal

Table 4. Comparison of critical SNR and average sensing time (case 4).

Sensing technique		Critical SNR ($P_d \geq 0.9$)	Average sensing time (ms)
Blind spectrum sensing	ED	–16 dB	0.0499
	MED	–16 dB	2.6
	CAV	–16 dB	2.5
	MME	–16 dB	2.9
Spectrum sensing based on prior knowledge	MFD	–30 dB	5.4
	LED	–18 dB	30.7
	FSC	–24 dB	0.0534

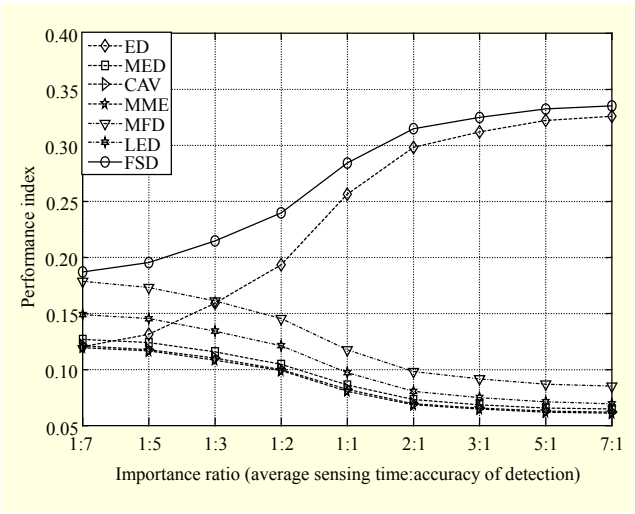

Fig. 7. Performance comparison using AHP algorithm.

and the coordinate system. We found that the weight vector effectively represents the WM signal, especially when SNR is

higher than –18 dB. When SNR is lower than –18 dB, where noise power is much greater than the WM signal power, the weight vector is contaminated with noise. Hence, the magnitude of the weight of correspondence between the received signal and the coordinate system is lower than the predetermined FSC threshold, which causes misdetection.

However, $P_{d(FSC)}$ is still higher than the P_d of other conventional techniques, including ED, MED, CAV, MME, and LED. This is because the effect of the noise on the weight vector is less than that on the WM signal.

To evaluate the trade-off between $P_{m(FSC)}$ and $P_{fa(FSC)}$, $P_{m(FSC)}$ is plotted as a function of $P_{fa(FSC)}$, as shown in Fig. 6(b). It should be noted that $P_{m(FSC)}$ is greater than 0 when the SNR is lower than –18 dB; hence, $P_{m(FSC)}$ at three different SNRs — –20 dB, –26 dB, and –30 dB — is shown. From Fig. 6(b), it can be seen that $P_{m(FSC)}$ slightly decreases when $P_{fa(FSC)}$ increases, which is similar to what happens in the cases of the other conventional techniques.

To evaluate the overall performances of the spectrum sensing techniques, we combine two performance metrics, P_d and average sensing time of each technique, using a standard multi-criteria ranking technique — analytic hierarchy process [28]. In the first step, we have to determine the importance ratio between P_d and average sensing time, which has never been standardized. Herein, the importance ratios are set as follows: 1:7, 1:5, 1:3, 1:2, 1:1, 2:1, 3:1, 5:1, and 7:1. It should be noted that the importance ratio of 1:7 means that the P_d is 7 times more important than the average sensing time, while 7:1 means the P_d is 7 times less important than the average sensing time. As shown in Fig. 7, the FSC algorithm gives the highest overall performance at any weight of importance. The reason is that the FSC algorithm gives a high rate of detection while utilizing a short sensing time.

V. Conclusion

In this paper, a novel spectrum sensing algorithm, fast spectrum sensing with coordinate system (FSC), is proposed. The FSC extracts only the significant features of the WM signals to build a new coordinate system. The FSC algorithm determines the existence of a PU by comparing the FSC decision statistic to the FSC threshold. Using our new coordinate system, the FSC requires less space for SU's knowledge base compared to that of other knowledge-based techniques. By measuring the magnitude of the weight of correspondence between the received signal and the coordinate system, FSC performs spectrum sensing with little computational burden and utilizes a short sensing time, while offering a detection accuracy close to that of MFD. The FSC can be well implemented by an SU, when the patterns of the PU signal are known to the SU, with much less computational complexity and sensing time than any of the other knowledge-based spectrum sensing techniques considered in this paper. Moreover, FSC is appropriate for real-time application because it uses a sensing time that is as short as that of ED.

Acknowledgement

The authors would like to thank our mentor, Assoc. Prof. Pornchai Supnithi, for the many times he spared some of his time just to give useful advice.

References

[1] A.M. Wyglinski, M. Nekovee, and Y.T. Hou, "*Cognitive Radio Communications and Networks: Principles and Practice*," Burlington, MA, USA: Elsevier Science Ltd, 2009.

[2] I.F. Akyildiz et al., "A Survey on Spectrum Management in Cognitive Radio Networks," *IEEE Commun. Mag.*, vol. 46, no. 4, Apr. 2008, pp. 40–48.

[3] R. Ranganathan et al., "Cognitive Radio for Smart Grid: Theory, Algorithms, and Security," *Int. J. Digital Multimedia Broadcast.*, vol. 2011, 2011.

[4] I.F. Akyildiz, W.-Y. Lee, and K.R. Chowdhury, "CRAHNs: Cognitive Radio Ad Hoc Networks," *Ad Hoc Netw.*, vol. 7, no. 5, July 2009, pp. 810–836.

[5] Y. Liang et al., "Cognitive Radio Networking and Communications: An Overview," *IEEE Trans. Veh. Technol.*, vol. 60, no. 7, Sept. 2011, pp. 3386–3407.

[6] I.F. Akyildiz et al., "Next Generation/Dynamic Spectrum Access/Cognitive Radio Wireless Networks: A Survey," *Comput. Netw.*, vol. 50, no. 13, Sept. 2006, pp. 2127–2159.

[7] B. Wang and K.J.R. Liu, "Advances in Cognitive Radio Networks: A Survey," *IEEE J. Sel. Topics Signal Process.*, vol. 5, no. 1, Feb. 2011, pp. 5–23.

[8] C. Cordeiro et al., "IEEE 802.22: An Introduction to the First Wireless Standard Based on Cognitive Radios," *J. Commun.*, vol. 1, no. 1, 2006, pp. 38–47.

[9] S.J. Shellhammer and G. Chouinard, "Spectrum Sensing Requirements Summary," IEEE 802.22-06/0089rl, June 2006.

[10] T. Yucek and H. Arslan, "A Survey of Spectrum Sensing Algorithms for Cognitive Radio Applications," *IEEE Commun. Surveys Tutorials*, vol. 11, no. 1, 2009, pp. 116–130.

[11] L. Lu et al., "Ten Years of Research in Spectrum Sensing and Sharing in Cognitive Radio," *EURASIP J. Wireless Commun. Netw.*, Jan. 2012, pp. 28–43.

[12] A. Bagwari and B. Singh, "Comparative Performance Evaluation of Spectrum Sensing Techniques for Cognitive Radio Networks," *Int. Conf. CICN*, Mathura, India, Nov. 3–5, 2012, pp. 98–105.

[13] S.A. Malik et al., "Comparative Analysis of Primary Transmitter

Detection Based Spectrum Sensing Techniques in Cognitive Radio Systems," *Australian J. Basic Appl. Sci.*, vol. 4, no. 9, 2010, pp. 4522–4531.

[14] H. Yousry et al., *Wireless Microphone Sensing Using Cyclostationary Detector*. Accessed June 16, 2012. http://conf-scoop.org/inct-2012/14_yousry_Hatem.pdf

[15] W. Ejaz et al., "Improved Local Spectrum Sensing for Cognitive Radio Networks," *EURASIP J. Adv. Signal Process.*, vol. 2012, Nov. 2012, pp. 242–251.

[16] A.K. Dey and A. Banerjee, "On Primary User Detection Using Energy Detection Technique for Cognitive Radio," *National Conf. Commun.*, Guwahati, India, Jan. 16–18, 2009.

[17] Y. Zeng, C. Koh, and Y. Liang, "Maximum Eigenvalue Detection: Theory and Application," *IEEE Int. Conf. Commun.*, Beijing, China, May 19–23, 2008, pp. 4160–4164.

[18] Y. Zeng and Y. Liang, "Spectrum-Sensing Algorithms for Cognitive Radio Based on Statistical Covariances," *IEEE Trans. Veh. Technol.*, vol. 58, no. 4, May 2009, pp. 1804–1815.

[19] D. Simunic and T.S. Dhope, "Hybrid Detection Method for Spectrum Sensing in Cognitive Radio," *Proc. Int. Convention MIPRO*, Opatija, Croatia, May 21–25, 2012, pp. 765–770.

[20] A. Mate, K.-H. Lee, and I.-T. Lu, "Spectrum Sensing Based on Time Covariance Matrix Using GNU Radio and USRP for Cognitive Radio," *IEEE Long Island Syst. Appl. Technol. Conf.*, Farmingdale, NY, USA, May 6, 2011, pp. 1–6.

[21] Y. Zeng and Y. Liang, "Maximum-Minimum Eigenvalue Detection for Cognitive Radio," *IEEE Int. Symp. PIMRC*, Athens, Greece, Sept. 3–7, 2007, pp. 1–5.

[22] Y. Zeng and Y.C. Liang, "Eigenvalue-Based Spectrum Sensing Algorithms for Cognitive Radio," *IEEE Trans. Commun.*, vol. 57, no. 6, June 2009, pp. 1784–1793.

[23] A.T. Teshome, "*FPGA-Based Eigenvalue Detection Algorithm for Cognitive Radio*," M.S. thesis, Dept. of Electron., Eng., University of Gävle, Sweden, 2010.

[24] P. Zhang and R.C. Qiu, "GLRT-Based Spectrum Sensing with Blindly Learned Feature under Rank-1 Assumption," *IEEE Trans. Commun.*, vol. 61, no. 1, Jan. 2013, pp. 87–96.

[25] C. Clanton, M. Kenkel, and Y. Tang, "Wireless Microphone Signal Simulation Method," IEEE 802.22-07/0124r0, Mar. 2007.

[26] L.I Smith, *A Tutorial on Principal Component Analysis.*, Accessed Feb. 26, 2012. http://www.cs.otago.ac.nz/cosc453/student_tutorials/principal_ components.pdf

[27] K. Srisomboon et al., "A Performance Comparison of Two PWS Filters in Different Domain for Image Reconstruction Technique under Different Image Types," *Int. Conf. ECTI-CON*, Hua Hin, Thailand, May 16–18, 2012, pp. 168–171.

[28] *Introductory Mathematics of the Analytic Hierarchy Process*. Accessed Sept. 25, 2012. http://www.business.pitt.edu/faculty/papers/saaty-into-to-ahp-mathematics.pdf

Wilaiporn Lee received her BEng degree in electrical engineering from Khonkaen University, Thailand, in 2002 and her MEng and PhD degrees in electrical engineering from Chulalongkorn University, Bangkok, Thailand, in 2005 and 2008, respectively. She is now an assistant professor in electrical engineering at the Communication and Computer Network Research Group, Department of Electrical and Computer Engineering, King Mongkut's University of Technology North Bangkok, Thailand. Her research interests include image processing, ultra-wideband communication, cognitive radio communication, and smart grid communication.

Kanabadee Srisomboon received his BS degree in aviation electronics from the Civil Aviation Training Center, Thailand, in 2011 and his MEng degree in electrical engineering from King Mongkut's University of Technology North Bangkok, Thailand, in 2013. He is now pursuing his PhD degree in electrical engineering at the Communication and Computer Network Research Group, Department of Electrical and Computer Engineering, Faculty of Engineering, King Mongkut's University of Technology North Bangkok, Bangkok, Thailand. His research interests include image processing, smart grid communication, and cognitive radio communication.

Akara Prayote received his BSc degree in computer science from King Mongkut's Institute of Technology North Bangkok, Thailand, his MSc degree in computer science from the Asian Institute of Technology, Thailand, and his PhD degree in computer science and engineering from the University of New South Wales, AU. He is currently a lecturer with the Department of Computer and Information Science, King Mongkut's University of Technology North Bangkok, Thailand. He has published papers on applied artificial intelligence and ad hoc networks and communications. His research interests relate to ad hoc networks and communications; artificial intelligence; and problem solving.